ACI STRUCTURAL JOURNAL TECHNICAL PAPER

Title no. 87-S21

Nonlinear Analysis of Cracked Reinforced Concrete

by Hsuan-Teh Hu and William C. Schnobrich

A nonlinear material model for cracked reinforced concrete subjected to inplane shear and normal stresses has been developed. As a result, a set of constitutive equations suitable for incremental finite element analysis is derived. Features of the present model include the smeared crack representation, rotating crack approach, tension stiffening, stress degrading effect for concrete parallel to the crack direction, and shear retention of concrete on the crack surface. This material model has been tested against the experimental data of Vecchio and Collins and it has been demonstrated that this material model is adequate in describing the post-cracking behavior of reinforced concrete.

Keywords: cracking (fracturing); finite element method; **reinforced concrete;** shear properties; stiffness; stresses; stress-strain relationships; **structural analysis; tension.**

Reinforced concrete is by far one of the most commonly used construction materials. Because concrete is relatively weak and brittle in tension, concrete cracking as well as the interactions between steel and cracked concrete can cause highly nonlinear behavior in some reinforced concrete structures. Today, with the help of computers, it is possible to carry out a finite element analysis simulating such nonlinear behavior. However, the success of such an analysis depends on a thorough understanding and modeling of the composite material behavior.

Many important classes of structures, such as panels, walls, slabs and shells, can be approximated as being in a state of plane stress. This paper focuses on the constitutive modeling of cracked reinforced concrete elements under plane stress conditions. Based on the smeared crack representation,[1] a rotating crack approach is used in formulating the constitutive matrix for cracked concrete. Tension stiffening, a stress degrading effect for concrete parallel to the crack direction, and the shear retention phenomenon are all discussed briefly. Finally, the post-cracking constitutive equations for reinforced concrete are established and tested against the experimental data of Vecchio and Collins.[2]

Though concern has been expressed as to the validity of this model in Reference 3, it is noted there that this model is rotationally invariant. Furthermore, questions are raised about the rotation of physical defects in a material. However, the view that should be adopted is that the cracks defined by this model are not cracks in the strict sense, but rather notational cracks defining the average crack direction after the stress redistribution of the entire structure.

For a number of structural elements such as walls, plates, and shells, the need exists to define behavior beyond the basic linear regime. The determination of redistribution characteristics, basic failure modes, or patterns are the sorts of things that one might wish to establish. To proceed entails some definition of the nonlinear characteristics of the material. Precise point conditions are not important; more global section properties are adequate to establish such overall behavioral characteristics. Analyses that incorporate such refinements as fracture mechanics, concern about crack localization, etc. are unneeded expenses. The material model presented in this paper is considered precise enough to address plate and shell problems with the objective of investigating basic overall behavior.

CONSTITUTIVE MATRIX FOR REINFORCING STEEL

Reinforcing steel is treated as an equivalent uniaxial layered material placed at the depth of the centerline of the bars and smeared out horizontally over the region of bar effect (Fig. 1). As many layers are used as there are layers of bars in the cross section. The stress-strain curve of reinforcing steel is modeled by an idealized bilinear curve identical in tension and compression (Fig. 2). The dowel action of the reinforcing steel is neglected and the bond between steel and concrete is assumed to remain perfect. The incremental constitutive matrix for the ith steel layer C_{si} in the material coordinates x', y', as shown in Fig. 1, can be written as

ACI Structural Journal, V. 87, No. 2, March-April 1990.
Received Feb. 6, 1989, and reviewed under Institute publication policies.

Hsuan-Teh Hu is a research associate in the National Center for Composite Materials Research at the University of Illinois, Urbana. He received his PhD degree from the University of Illinois in 1988. His research interests include finite element analysis of reinforced concrete and the optimization of laminated composite structures.

William C. Schnobrich, FACI, is a professor of civil engineering at the University of Illinois, Urbana. His primary area of specialization is shell structures. He is a member of ACI-ASCE Joint Committee 334, Concrete Shell Design and Construction, and is chairman of the ASCE Committee on Finite Element Analysis of Reinforced Concrete.

$$[C]_{si} = \begin{bmatrix} \rho_i E_s & 0 & 0 \\ 0 & 0 & 0 \\ 0 & 0 & 0 \end{bmatrix} \quad (1)$$

where ρ_i and E_s are the steel percentage and the modulus of elasticity of the reinforcement in the ith layer. When yielding of steel occurs, the incremental constitutive matrix reverts to

$$[C]_{si} = \begin{bmatrix} \rho_i E_{sp} & 0 & 0 \\ 0 & 0 & 0 \\ 0 & 0 & 0 \end{bmatrix} \quad (2)$$

where E_{sp} is the plastic modulus for steel.

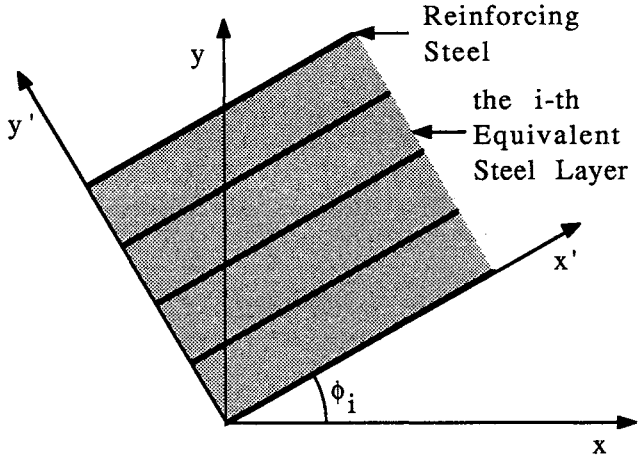

Fig. 1 — Equivalent steel layer and material coordinates for steel

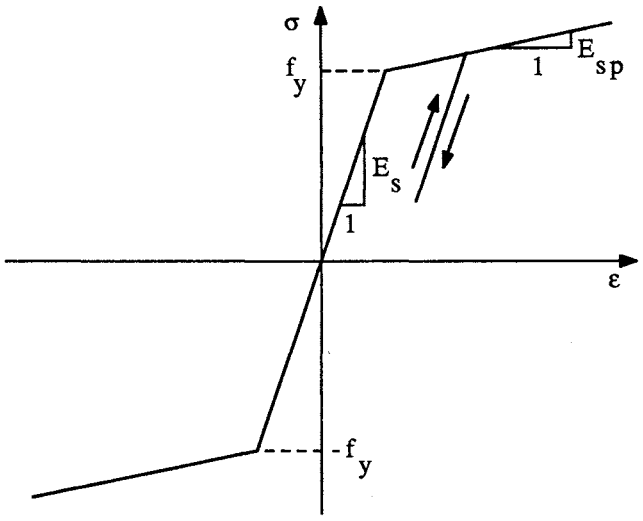

Fig. 2 — Idealized stress-strain curve for steel

ELASTIC CONCRETE

When the computed concrete stress lies inside the failure surfaces (Fig. 3), the behavior of concrete can be considered as purely elastic and the incremental stress-strain relationships for concrete can be written as

$$[C]_c = \frac{E_c}{1-\nu^2} \begin{bmatrix} 1 & \nu & 0 \\ 2\nu & 1 & 0 \\ 0 & 0 & \frac{1-\nu}{2} \end{bmatrix} \quad (3)$$

in which E_c is the initial modulus of elasticity for concrete and ν is its Poisson's ratio.

SINGLY CRACKED CONCRETE

In this study, a smeared crack model[1] is adopted. Within this model the initiation of a cracking process at any location happens when the concrete stresses reach one of the failure surfaces either in the biaxial tension region or in a combined tension-compression region. In the biaxial tension region, this surface is defined as[4]

$$c\left[\left(\frac{3}{2\sqrt{2}}\right)\left(\frac{1+\alpha}{\alpha}\right)\tau_{oct} + \left(\frac{3}{2}\right)\left(\frac{1-\alpha}{\alpha}\right)\sigma_m\right] - f'_c = 0 \quad (4)$$

with

$$\alpha = f'_t / f'_c$$

$$\tau_{oct} = \frac{\sqrt{2}}{3}\sqrt{\sigma_x^2 - \sigma_x\sigma_y + \sigma_y^2 + 3\tau_{xy}^2}$$

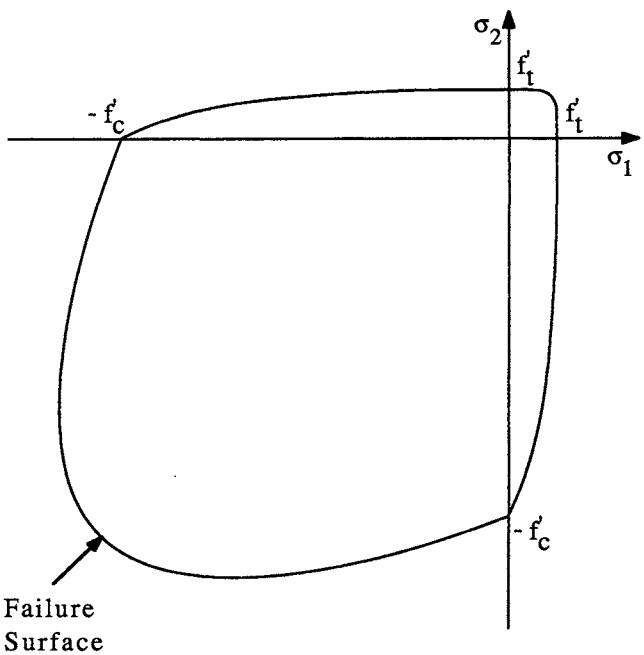

Fig. 3 — Failure surface of concrete in the two dimensional principal stress plane

$$\sigma_m = \frac{1}{3}(\sigma_x + \sigma_y)$$

and

$$c = 1 - 0.4019(\sigma_2/\sigma_1) + 0.008913(\sigma_2/\sigma_1)^2$$

where f_c' is the maximum compressive strength of concrete and f_t' is the maximum tensile strength of concrete. The quantities σ_1 and σ_2 are the maximum and the minimum principal stresses for concrete.

In the combined tension-compression region the failure surface is defined as

$$c\left[\left(\frac{3}{2\sqrt{2}}\right)\left(\frac{1+\alpha}{\alpha}\right)\tau_{oct} + \left(\frac{3}{2}\right)\left(\frac{1-\alpha}{\alpha}\right)\sigma_m\right] - f_c' = 0$$

where for $-\infty < \sigma_1/\sigma_2 < -0.103$

$$c = 1 - 0.02886(\sigma_2/\sigma_1) - 0.006657(\sigma_2/\sigma_1)^2 - 0.0002443(\sigma_2/\sigma_1)^3$$

and for $-0.103 \leqslant \sigma_1/\sigma_2 < 0$

$$c = 1 + 6.339(\sigma_1/\sigma_2) + 68.82(\sigma_1/\sigma_2)^2 + 183.8(\sigma_1/\sigma_2)^3$$

With the smeared crack representation, concrete is treated as an orthotropic material with principal axes normal and parallel to the crack direction (Fig. 4). The incremental stress-strain relationships associated with the crack coordinates then become

$$C' = \begin{bmatrix} 0 & 0 & 0 \\ 0 & E_t & 0 \\ 0 & 0 & \mu G_c \end{bmatrix} \quad (6)$$

where E_t is the tangent modulus of concrete parallel to the crack direction (choice of values discussed later). μ is the shear retention factor with $0 < \mu \leqslant 1$ (also discussed later). $G_c = E_c/2$ is the shear modulus of cracked concrete. The Poisson's ratio ν is taken as zero due to the lack of interaction between the two orthogonal directions.

TENSION STIFFENING

The use of the orthotropic constitutive Eq. (6) to represent cracked concrete may not be totally realistic, because the cracked concrete of a reinforced concrete element can still carry some tensile stress in the direction normal to the crack. This phenomenon is termed tension stiffening.[5,6] In this study, a general tension stiffening curve suggested by Bhide[7] is used. This curve is given as follows

$$f_t = \frac{f_t'}{1 + 1000\,\epsilon_t(|\phi|/90)^{1.5}} \quad (7)$$

where f_t and ϵ_t are the average tensile stress and the average tensile strain normal to the crack direction. ϕ is measured in degrees counterclockwise from the steel direction to the crack direction. In the case of unequal reinforcement in two orthogonal directions, the axis of the stronger reinforcement is taken as the reference direction. Eq. (7) is plotted for various values of ϕ in Fig. 5.

In situations where the reinforcing steel yields, the average tensile stress of cracked concrete is close to zero.[2] Therefore, the tension-stiffening effect should not artificially increase the total stress in the direction of any yielded reinforcement; otherwise, an overestimation of the ultimate capacity may be expected. If there are N layers of steel existing at a concrete section, then a generalized upper bound for the concrete tension-stiffening stress can be written as

$$f_t \leqslant \sum_{i=1}^{N} \rho_i (f_{yi} - f_{si}) \cos^2 \theta_i \quad (8)$$

in which f_{si} and f_{yi} are current stress (in tension) and yield stress, respectively, for the ith steel layer. θ_i is measured couterclockwise from ith steel axis to the direction normal to crack.

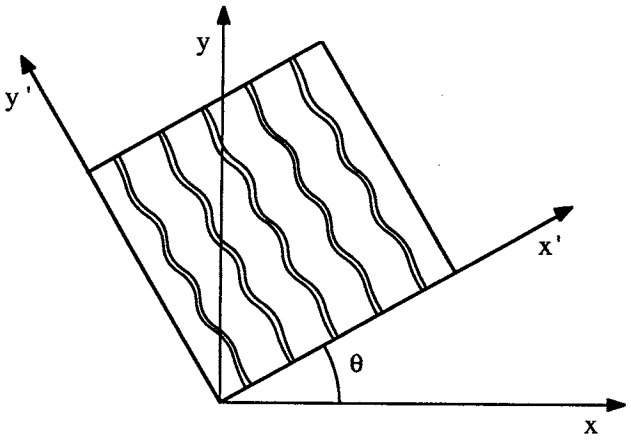

Fig. 4 — Crack coordinates

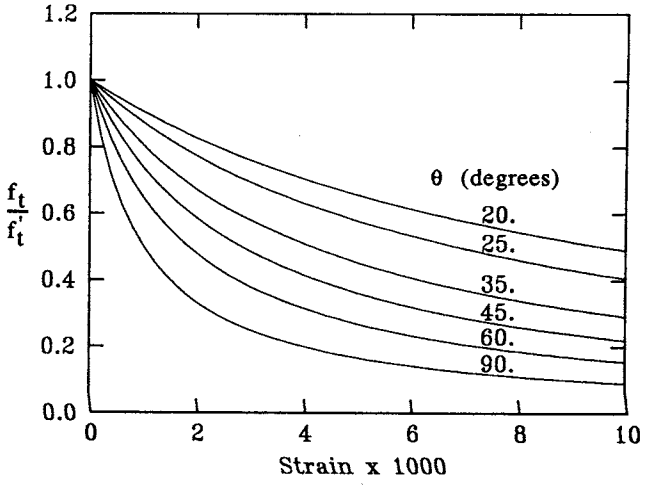

Fig. 5 — Tension-stiffening curves suggested by Bhide

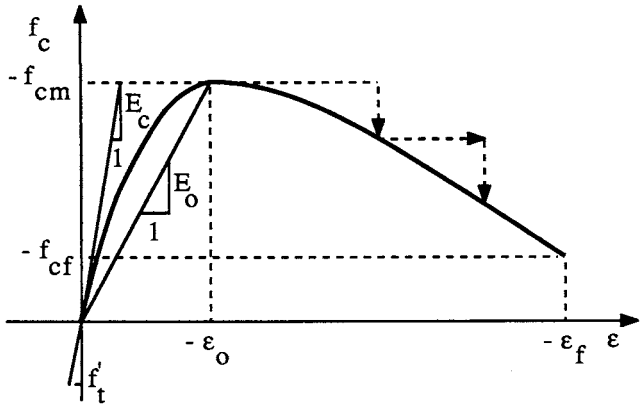

Fig. 6 — Stress-strain curve for concrete parallel to the crack direction

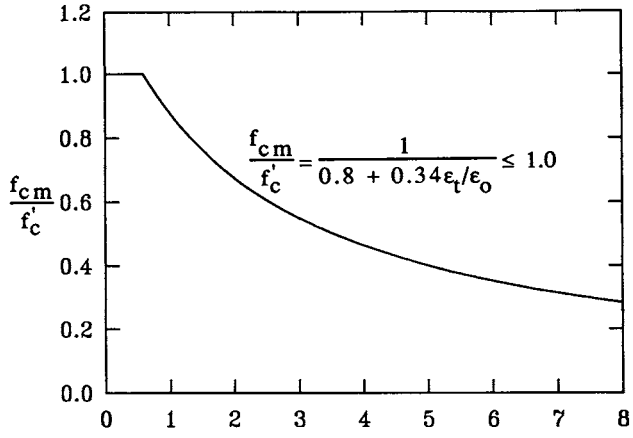

Fig. 7 — Degraded maximum compressive strength for cracked concrete

STRESS DEGRADING EFFECT FOR CONCRETE PARALLEL TO CRACK DIRECTION

After cracking has taken place, the concrete parallel to the crack direction is still capable of resisting either tensile or compressive forces. When it is subjected to tension, a pure linear-elastic behavior is assumed (Fig. 6) and E_t is taken as E_c in Eq. (6). On the other hand, when it is subjected to compression, experimental results[2,8] show that the tensile cracks have caused damage to the concrete with the transverse tensile strain, having a degrading effect not only on the compressive strength but also on the compressive stiffness. Therefore, concrete in this situation is softer, with weaker values than those recorded from a standard cylinder test.

Several formulas[2,9,10] have been proposed to determine the degraded maximum compressive strength f_{cm} for concrete parallel to the crack direction and the experimentally determined relationship suggested by Vecchio and Collins[10] is used in this study (Fig. 7). That is

$$\frac{f_{cm}}{f'_c} = \frac{1}{0.8 + 0.34\epsilon_t/\epsilon_o} \leqslant 1.0 \qquad (9)$$

where ϵ_o is the strain corresponding to the maximum concrete compressive strength f'_c. After the peak strength f_{cm} is determined, the widely used stress-strain curve suggested by Saenz[11] is employed to calculate the concrete compressive stress f_c. We have (Fig. 6)

$$f_c = \frac{E_c\epsilon}{1 + (R+R_E-2)\left(\frac{\epsilon}{\epsilon_o}\right) - (2R-1)\left(\frac{\epsilon}{\epsilon_o}\right)^2 + R\left(\frac{\epsilon}{\epsilon_o}\right)^3} \qquad (10)$$

in which

$$R = \frac{R_E(R_\sigma - 1)}{(R_\epsilon - 1)^2} - \frac{1}{R_\epsilon}$$

$$R_E = \frac{E_c}{E_o}$$

$$R_\sigma = \frac{f_{cm}}{f_{cf}}$$

$$R_\epsilon = \frac{\epsilon_f}{\epsilon_o}$$

and

$$E_o = \frac{f_{cm}}{\epsilon_o}$$

For f_{cf} and ϵ_f, Hu and Schnobrich[4] used $R_\sigma = 4$ and $R_\epsilon = 4$; Darwin and Pecknold[12] used $R_\sigma = 5$ and $R_\epsilon = 4$. Generally, to define σ_f and ϵ_f on any rigorous experimental basis is impossible because the descending branch of the stress-strain curve is highly test-dependent and is usually unavailable from statically determinate tests. In this study, it is assumed that $R_\sigma = 4$ and $R_\epsilon = 4$.

The tangent modulus E_t used in Eq. (6) can then be calculated by differentiating Eq. (10)

$$E_t = \frac{df_c}{d\epsilon} = \frac{E_c\left[1 + (2R-1)\left(\frac{\epsilon}{\epsilon_o}\right)^2 - 2R\left(\frac{\epsilon}{\epsilon_o}\right)^3\right]}{\left[1 + (R+R_E-2)\left(\frac{\epsilon}{\epsilon_o}\right) - (2R-1)\left(\frac{\epsilon}{\epsilon_o}\right)^2 + R\left(\frac{\epsilon}{\epsilon_o}\right)^3\right]^2} \qquad (11)$$

It should be noted that, due to degrading of the maximum compressive strength, the tangent modulus is also reduced simultaneously. To prevent the numerical difficulty associated with negative tangent moduli, once the peak stress f_{cm} has been reached, E_t is set to zero and the unbalanced stresses are released in a stepwise fashion (Fig. 6).

SHEAR RETENTION FACTOR

After cracking has taken place, cracked reinforced concrete can still transfer shear forces through aggregate interlock or shear friction and dowel action. To

take the shear stiffness of cracked concrete into account in the smeared crack model, a reduced shear modulus μG_c is retained (with $0 < \mu \leqslant 1$) in the constitutive Eq. (6) instead of dropping that capacity to zero. Using a reduced shear modulus not only improves the realism of the cracking representation during the finite element analysis but also removes most of the numerical difficulties caused by the singularity of the composite material's constitutive matrix.[6]

Various forms of the shear retention factor have been proposed.[6] However, numerous analytical results have demonstrated that the particular value chosen for μ (between 0 and 1) does not appear to be critical, but values greater than zero are necessary to prevent numerical instabilities.[4,6] Consequently, a constant value of $\mu = 0.25$ is used in this investigation.

DOUBLY CRACKED CONCRETE

Upon further loading of singly cracked concrete, a second set of cracks can form in the direction normal to the first set of smeared cracks. Therefore, in that direction, if the concrete stress is less than f'_t, then concrete remains singly cracked. Otherwise, if it is greater than f'_t, then the second set of cracks forms. The constitutive matrix for doubly cracked concrete is written

$$[C'] = \begin{bmatrix} 0 & 0 & 0 \\ 0 & 0 & 0 \\ 0 & 0 & \mu G_c \end{bmatrix} \tag{12}$$

and the tension stiffening stresses normal to both crack directions can be calculated by using Eq. (7).

CONSTITUTIVE MATRIX FOR CRACKED CONCRETE

In most conventional finite element analyses of reinforced concrete structures, crack directions are assumed fixed once they form and while they remain open. This conception is termed the "fixed crack model" and has been used by many investigators.[6] However, this model leads to crack directions that can be inconsistent with the limit state.[13] The change in the crack direction and the consequential change in direction of the maximum stiffness were clearly observed in the experiments of Vecchio and Collins.[2] Therefore, the need for an algorithm that can account for this rotating crack effect is obvious.

The rotating crack concept for finite element analysis of reinforced concrete was first introduced by Cope and Rao.[14] The basic assumption for this approach is that after cracking takes place, the crack direction is always perpendicular to the direction of the major principal strain axis during the course of loading. This concept has been further extended by Gupta and Akbar[13] by obtaining the rotating crack tangent stiffness matrix as the sum of the conventional tangent constitutive matrix for cracked concrete, plus a contribution that represents the effect of the possible changes in crack direction. This can be written as

$$\begin{aligned} \Delta\{\sigma\} &= [C]_f \Delta\{\epsilon\} + \frac{d\{\sigma\}}{d\theta} d\theta \\ &= \{[C]_f + [G]\}\Delta\{\epsilon\} \end{aligned} \tag{13}$$

in which $[C]_f$ is the constitutive matrix for a fixed crack model while $[G]$ reflects the possible changes in the crack direction.

The rotating crack model developed by Gupta and Akbar[13] has been further modified by Milford and Schnobrich[15] and Hu and Schnobrich[4] by taking account of the nonlinearity of concrete in compression while including tensile stiffening and shear retention for the cracked concrete. The constitutive matrix used in this analysis has been detailedly derived in Reference 4. This matrix has the following form

$$[C]_c = [T(\theta)]^T[C'][T(\theta)] + [G] \tag{14}$$

where

$$[T(\theta)] = \begin{bmatrix} \cos^2\theta & \sin^2\theta & \sin\theta\cos\theta \\ \sin^2\theta & \cos^2\theta & -\sin\theta\cos\theta \\ -2\sin\theta\cos\theta & 2\sin\theta\cos\theta & \cos^2\theta - \sin^2\theta \end{bmatrix} \tag{15}$$

$$[G] = \frac{(\sigma_{x'} - \sigma_{y'})\cos^2 2\theta}{2(\epsilon_x - \epsilon_y)} \begin{bmatrix} \sin^2 2\theta & -\sin^2 2\theta & -\sin 2\theta\cos 2\theta \\ -\sin^2 2\theta & \sin^2 2\theta & \sin 2\theta\cos 2\theta \\ -\sin 2\theta\cos 2\theta & \sin 2\theta\cos 2\theta & \cos^2 2\theta \end{bmatrix} \tag{16}$$

and θ is measured counterclockwise from global x-axis to crack x'-axis (Fig. 4).

For singly cracked concrete, $[C']$ in Eq. (14) can be calculated by Eq. (6). $\sigma_{x'}$ and $\sigma_{y'}$ in Eq. (16) are the tension-stiffening stress normal to the crack direction and the concrete stress parallel to the crack direction, respectively. For doubly cracked concrete, $[C']$ in Eq. (14) can be calculated by Eq. (12). $\sigma_{x'}$ and $\sigma_{y'}$ in Eq. (16) are the tension-stiffening stresses normal to the first crack and the second crack directions.

CONSTITUTIVE MATRIX FOR REINFORCED CONCRETE

The total material stiffness matrix for reinforced concrete $[C]_{rc}$ is the sum of the component matrices of concrete and steel and can be written

$$[C]_{rc} = [C]_c + \sum_{i=1}^{N} [T(\phi_i)]^T[C]_{si}[T(\phi_i)] \tag{17}$$

where $[C]_c$ can be determined by using Eq. (3) or (14). $[C]_{si}$ can be determined by using Eq. (1) or (2) and ϕ_i is the direction angle of the ith reinforcement (Fig. 1).

COMPARISON WITH EXPERIMENTAL RESULTS

The response of reinforced concrete panels subjected to inplane shear and normal stresses has been extensively investigated by Vecchio and Collins.[2] The test panels were 890 mm (35 in.) and 70 mm (2.75 in.) thick

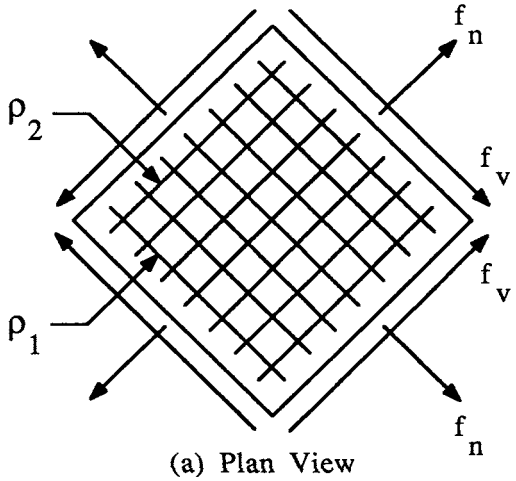

(a) Plan View

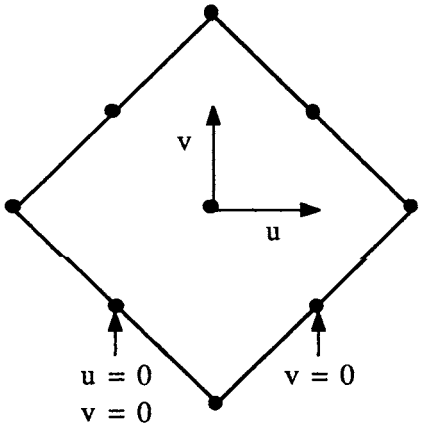

(b) Finite Element Idealization

Fig. 8 — Vecchio-Collins specimens

and were reinforced with welded wire mesh. The plan view of reinforcing steel and loading directions are shown in Fig. 8(a). The finite element idealization for the test specimen is shown in Fig. 8(b), where a fully integrated nine-node isoparametric element is used to model the reinforced concrete panel. To solve the nonlinear equilibrium equations, the incremental iterative Newton-Raphson scheme is employed.

A list of the analyzed panels along with concrete properties and steel information are given in Table 1. The following material properties are assumed in the analysis: $f_t' = 0.33\sqrt{f_c'}$ MPa; $E_c = 4730\sqrt{f_c'}$ MPa; $E_s = 200{,}000$ MPa; $E_{sp} = 0.01E_s$; and $\nu = 0.19$. All these panels are subjected to pure shear up to failure. One exception is panel PV28, which is subjected to combined tension and shear with the f_n/f_v ratio being fixed and equal to 0.32.

The failure mechansims for the panels analyzed in this study fall into three categories, namely: (1) steel yielding in both directions (SY); (2) concrete failure after yielding of the weaker reinforcement but prior to yielding of the stronger reinforcement (C1); and (3) concrete failure prior to yielding of any reinforcement (C2). To carefully examine the stress-degrading effect parallel to the crack direction and the influence of tension stiffening, three panels—PV11, PV19, and PV22—which cover the three failure modes mentioned above, are investigated through the numerical simulation.

The results for panels PV11, PV19, and PV22 are plotted in Fig. 9. For panel PV11 the failure mode is SY. Both the (a) and (b) calculated solutions, which exclude tension-stiffening stress, still predict the ultimate

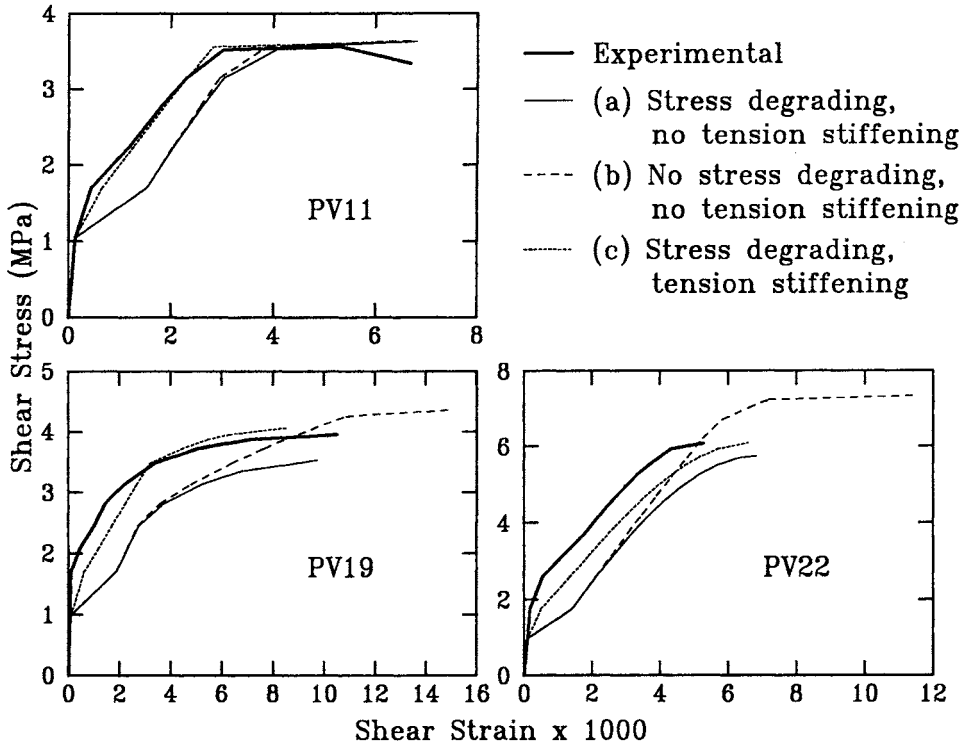

Fig. 9 — Verification of stress-degrading effect and tension stiffening (1 MPa = 0.145 ksi)

load and failure mechanism accurately. Because the level of tensile strain normal to the crack is relatively small compared with ϵ_o, there is no severe damage to the concrete in the direction parallel to the crack and, therefore, the stress-degrading effect is not prominent in this specimen.

For Panels PV19 and PV22, the failure modes are C1 and C2, respectively. The solution (a) predicts the failure mechanisms correctly for both panels. Although the calculated ultimate loads are underestimated a little, the solution is still reasonable because the tension-stiffening stress has not been taken into account. On the other hand, the solution (b) not only overestimates the ultimate loads but also predicts the wrong failure mode SY for both panels. The discrepancy between solutions (a) and (b) for these two panels does show an influence from the stress-degrading effect.

On the base of the rotating crack model with stress-degrading effect, solution (c) in Fig. 9 is obtained by adding a tension-stiffening stress contribution to the concrete. In general, good agreement is obtained between solution (c) and the experimental results. By comparing (c) with solution (a), the predicted behavior of panels PV11, PV19, and PV22 is greatly improved by considering the tension stiffening after concrete cracking takes place.

Finally, the rotating crack model with stress-degrading effect and tension-stiffening stress applied to concrete is employed to analyze the remaining panels. Comparisons of the experimental response and the numerical results are shown in Fig. 10, while further details are given in Table 2. In general, the numerically predicted ultimate loads and the failure modes generated with these material models are in good agreement with the experimental results. The crack orientations at the final loading stage are also very consistent with the experimental data.

CONCLUSIONS

Based on a smeared crack representation coupled with the rotating crack approach, the presented

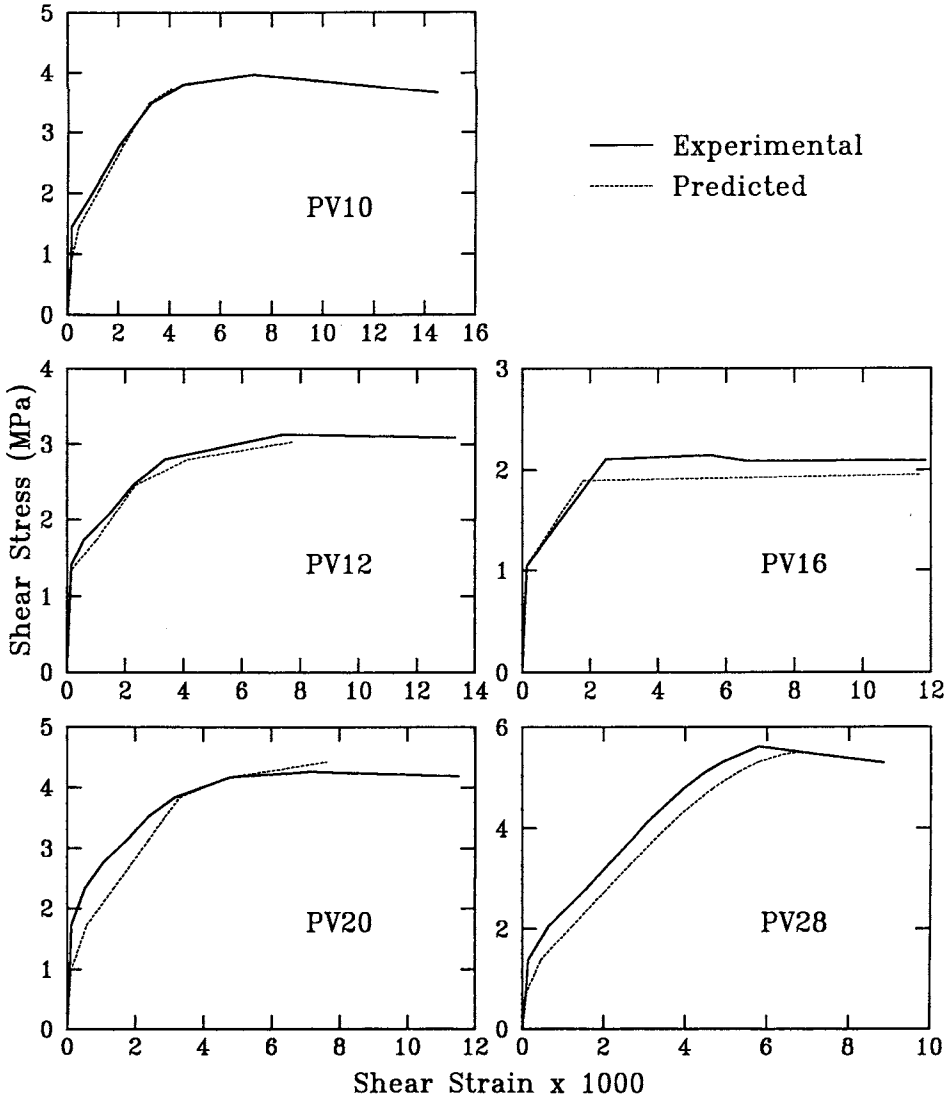

Fig. 10 — Comparison of experimental and numerical shear stress-strain curves (1 MPa = 0.145 ksi)

Table 1 — Material properties for Vecchio-Collins specimens

Panel	Steel				Concrete	
	ρ_1	ρ_2	f_{y1}, MPa	f_{y2}, MPa	ϵ_o	f'_c, MPa
PV10	0.01785	0.00999	276	276	0.00270	14.5
PV11	0.01785	0.01306	235	235	0.00260	15.6
PV12	0.01785	0.00446	469	269	0.00250	16.0
PV16	0.00740	0.00740	255	255	0.00200	21.7
PV19	0.01785	0.00713	458	299	0.00215	19.0
PV20	0.01785	0.00885	460	297	0.00180	19.6
PV22	0.01785	0.01524	458	420	0.00200	19.6
PV28	0.01785	0.01785	483	483	0.00185	19.0

1 MPa = 0.145 ksi.

Table 2 — Experimental and numerical results for Vecchio-Collins specimens

Panel	Experimental			Predicted		
	Failure mode	v_u, MPa	θ*	Failure mode	v_u, MPa	θ*
PV10	C1	3.97	52	C1	3.73	49
PV11	SY	3.56	50	SY	3.63	49
PV12	C1	3.13	58	C1	3.03	60
PV16	SY	2.14	45	SY	1.95	45
PV19	C1	3.96	57	C1	4.06	56
PV20	C1	4.26	54	C1	4.43	54
PV22	C2	6.07	45	C2	6.08	46
PV28	C2	5.80	45	C2	5.50	45

*Average orientation of maximum principal concrete stress and strain, measured counterclockwise in degrees from the weaker reinforcement direction.
1 MPa = 0.145 ksi.

constitutive model is capable of predicting the post-cracking behavior of reinforced concrete elements subjected to inplane shear and normal stresses. In addition, it has proved adequate in modeling the reinforced concrete elements, such as beam, plate, and shell, subjected to flexural forces.[4] There are several conclusions obtained from this study:

1. The inclusion of the stress-degrading effect for concrete parallel to the crack direction is crucial, especially for reinforced concrete panels that fail by concrete failure. This is important if the degradation observed in the experimental data actually carries over to real structures.

2. After concrete cracking takes place, applying the tension-stiffening stress to the concrete greatly improves the predicted behavior of the reinforced concrete panels, whether these panels fail either by concrete failure or by steel failure.

3. The proposed material model is a powerful tool that is easily programmed into a finite element analysis. All required input data are standard material properties; therefore, parameter study prior to the numerical analysis is not necessary.

ACKNOWLEDGMENTS

This work was financially supported by the National Science Foundation under grant number NSF CEE 83-00226.

NOTATION

$[C]_c$ = constitutive matrix of concrete in global coordinates
$[C]_f$ = constitutive matrix of concrete for fixed-crack model
$[C']$ = constitutive matrix of cracked concrete in crack coordinates
$[C]_{rc}$ = constitutive matrix of reinforced concrete in global coordinates
$[C]_{si}$ = constitutive matrix of ith steel layer in material coordinates
E_c = initial modulus of elasticity for concrete
E_s = modulus of elasticity of steel
E_{sp} = plastic modulus of steel
E_t = tangent modulus of concrete
f_c = compressive stress of concrete
f'_c = maximum compressive stress of concrete (positive quantity)
f_{cf} = stress corresponding to ϵ_f on the uniaxial stress-strain curve
f_{cm} = degraded maximum compressive stress of concrete (positive quantity)
f_n = normal stress
f_{si} = stress for ith steel layer
f_t = tensile stress of concrete
f'_t = maximum tensile strength of concrete
f_v = shear stress
f_{yi} = yield stress for ith steel layer
$[G]$ = matrix that reflects the possible changes in the crack direction
G_c = shear modulus of cracked concrete
$[T(\ )]$ = transformation matrix
(x,y) = global coordinates
(x',y') = material coordinates or crack coordinates
ϵ_o = strain corresponding to f'_c in an uniaxial compression test
ϵ_f = maximum compressive strain on the uniaxial stress-strain curve
ϵ_t = tensile strain of concrete
ρ_i = steel percentage for ith steel layer
ϕ = angle measured counterclockwise in degrees from strong reinforcement direction to crack direction
ϕ_i = angle between the ith reinforcement and the global x-axis
μ = shear retention factor
θ = rotational angle between the global coordinates and the crack coordinates
θ_i = angle between the ith steel axis and the direction normal to crack
ν = Poisson's ratio
σ_1 = maximum principal stress of concrete
σ_2 = minimum principal stress of concrete
$\sigma_x,\sigma_y,\tau_{xy}$ = stresses of concrete in global coordinates
σ_x',σ_y' = stresses of concrete in crack coordinates

REFERENCES

1. Rashid, Y. R., "Ultimate Strength Analysis of Prestressed Concrete Pressure Vessels," *Nuclear Engineering and Design* (Lausanne), V. 7, No. 4, Apr. 1968, pp. 334-344.

2. Vecchio, F., and Collins, M. P., "The Response of Reinforced Concrete to In-Plane Shear and Normal Stresses," *Publication* No. 82-03, Department of Civil Engineering, University of Toronto, Mar. 1982, 332 pp.

3. Bažant, Z. P., "Discussion of Session 2, Part 1," *Final Report,* IABSE Colloquium on Advanced Mechanics of Reinforced Concrete (Delft, June 1981), International Association for Bridge and Structural Engineering, Zürich, pp. 490-491.

4. Hu, H.-T., and Schnobrich, W. C., "Nonlinear Analysis of Plane Stress State Reinforced Concrete Under Short Term Monotonic Loading," Civil Engineering Studies, *Structural Research Series* No. 539, University of Illinois, Urbana, Apr. 1988, 238 pp.

5. ACI Committee 224, "Cracking of Concrete Members in Direct

Tension," (ACI 224.2R-86), American Concrete Institute, Detroit, 1986, 11 pp.

6. *Finite Element Analysis of Reinforced Concrete,* American Society of Civil Engineers, New York, 1982, 545 pp.

7. Bhide, S. B., "Reinforced Concrete Elements in Shear and Tension," PhD thesis, University of Toronto, 1986.

8. Maekawa, K., and Okamura, H., "The Deformational Behavior of Constitutive Equation of Concrete Using the Elasto-Plastic and Fracture Model," *Journal of the Faculty of Engineering* (University of Tokyo), V. 39, No. 2, 1983, pp. 253-328.

9. Cervenka, Vladimir, "Constitutive Model for Cracked Reinforced Concrete," ACI JOURNAL, *Proceedings* V. 82, No. 6, Nov-Dec. 1985, pp. 877-882.

10. Vecchio, Frank J., and Collins, Michael P., "The Modified Compression-Field Theory for Reinforced Concrete Elements Subjected to Shear," ACI JOURNAL, *Proceedings* V. 83, No. 2, Mar.-Apr. 1986, pp. 219-231.

11. Saenz, Luis P., Discussion of "Equation for the Stress-Strain Curve of Concrete" by Prakash Desayi and S. Krishnan, ACI JOURNAL, *Proceedings* V. 61, No. 9, Sept. 1964, pp. 1229-1235.

12. Darwin, D., and Pecknold, D. A., "Inelastic Model for Cyclic Biaxial Loading for Reinforced Concrete," Civil Engineering Studies, *Structural Research Series* No. 409, University of Illinois, Urbana, July 1974, 169 pp.

13. Gupta, A. K., and Akbar, H., "Cracking in Reinforced Concrete Analysis," *Journal of Structural Engineering,* ASCE, V. 110, No. 8, Aug 1984, pp. 1735-1746.

14. Cope, R. J., and Rao, P. Vasudeva, "Non-Linear Finite Element Analysis of Slab Structures," *Proceedings,* Institution of Civil Engineers (London), Part 2, V. 63, Mar. 1977, pp. 159-179.

15. Milford, R. V., and Schnobrich, W. C., "Nonlinear Behavior of Reinforced Concrete Cooling Towers," Civil Engineering Studies, *Structural Research Series* No. 514, University of Illinois, Urbana, May 1984, 192 pp.